Synthesis, DFT analysis and in-vitro anti-cancer study of novel fused bicyclic pyranone isoxazoline derivatives of Goniodiol-diacetate-a natural product derivative

Doddabasappa Talimarada [a], Akanksha Sharma [a], Mahesh G. Wakhradkar [b], Sundar N. Dhuri [c], Krishna Chaitanya Gunturu [b,*], Venkata Narayanan Naranammalpuram Sundaram [a], Harish Holla [a,*]

[a] Department of Chemistry, Central University of Karnataka, Kalaburagi 585367, India
[b] School of Chemical Sciences, S. R. T. M. University, Nanded, India
[c] School of Chemical Sciences, Goa University, Goa, India

ARTICLE INFO

ABSTRACT

Natural products, natural product-inspired molecules and natural product derivatives have contributed around 79% to the new chemotherapies against the most complex, deadly disease, cancer. In this study, a series of novel isoxazoline derivatives of Goniodiol diacetate (fused bicyclic pyranone isoxazoline derivatives)- a natural product derivative, were synthesized with quantitative yield as a single regioisomer by 1,3 - dipolar cycloaddition reaction with different aldoximes. The regiospecific product formed was confirmed by NOESY study and single-crystal X-ray diffraction. The regiospecificity of the product formation was further explained by co-efficients of selected atomic orbitals in frontier molecular orbitals and natural population analysis (NPA in eV) of dipolarophile and dipole by density functional theory studies. All the derivatives have demonstrated anti-cancer activity selectively in human breast cancer (MDA-MB-231), ovarian cancer (SKOV3), prostate cancer (PC-3) and colon cancer (HCT-15) cell lines with $EC_{50} < 10$ μM. Additionally, Annexin V/PI assay and cell cycle analysis on selected potent compound **3 f** exhibited tuned apoptotic response & necrosis compared to standard Vincristine and showed cell growth arrest at the S phase.

1. Introduction

One of the possible ways of drug discovery can be a generation of chemical libraries using natural product molecules (NPM) as scaffolds or as starting point. Natural products have displayed diverse pharmacological activities that are explored in treating various ailments [1–4]. Natural products contribute significantly to the treatment of one of the deadliest & complex diseases, i.e. Cancer. As per a recent review by Newmann and Cragg, there are in total 259 small molecules which have enacted antitumor activities, out of which 206 molecules are either natural products, natural product derivatives, natural product mimics or natural product inspired molecules, contributing to an astounding 79% in the new chemotherapies till 2019 [5]. These NPM's may act as active pharmaceutical ingredients (API) in the traditional medicine systems like Ayurveda or Traditional Chinese Medicine by synergistic effect with multiple concoctions of molecules in a lower dose. They are also

effective in modern medicines as single component multiple targeting agents.

In our endeavor to explore the α, β-unsaturated δ-lactone molecules from the natural origin, earlier we have reported a bioassay-guided fractionation study on the relatively less reported medicinal plant, *Goniothalamus wynaadensis* Bedd. [6] *Goniothalamus wynaadensis* Bedd. is an endemic species to the Southern region of India, belongs to the Annonaceae family, and is used for different disorders in folk medicine [7,8]. Different species of the Goniothalamus genus have been reported as part of herbal formulation in combination with other plant species for skin diseases, leukemia, various cancers like lung cancer, breast cancer, ovarian cancer etc., diabetes and gynecological disorders [9–11]. Several research groups have isolated structurally diverse styryl lactones comprising α, β-unsaturated δ-lactones in their structures from various species of genus *Goniothalamus* possessing various biological properties (Fig. 1) [12]. Apart from these, the lactone containing molecules like

Camptothecin, fused furano pyranolactones like Altholactones, Ortho-diffenes, and α, β-unsaturated δ-lactones like Pironetine are hit molecules in cancer chemotherapies and few of them are in clinical trials (Fig. 1) [13–19].

In our preliminary communication, we have reported ethyl acetate extract of the plant species *Goniothalamus wynaadensis* to be cytotoxic to a few cancer cell lines [6]. On further purification of the extract using column chromatography led to the known cytotoxic molecule Goniodiol-7-monoacetate (**1**) comprising α, β-unsaturated δ-lactone [20]. In order to enhance the bioactivity of the isolated molecules, synthetic derivatization with possible incorporation of a heterocyclic component to α, β-unsaturated δ-lactone of the isolated molecule was envisaged. These incorporations were expected to keep the δ-lactone intact in the structure and will create a fused bicyclic molecule. The α, β-unsaturated δ-lactone scaffold can act as an active dipolarophile and is prone to cycloaddition chemistry to synthesize fused bicyclic heterocyclic molecules. Incorporating isoxazolines by 1,3-dipolar cycloaddition chemistry was envisioned among the heterocycles, as isoxazolines are an important class of nitrogen and oxygen-containing heterocycles which are part of new chemical entities in the field of medicinal chemistry as the anti-cancer agents [21]. Apart from this, isoxazolines are important pharmacophore and structural building blocks of biologically active molecules from nature and synthesized libraries [22]. Some fused isoxazolines like chromeno isoxazolines have displayed anti-psychotic, anti-depressant and anti-anxiety activities (Fig. 2) [23]. Few bicyclic fused isoxazolines were reported to be trans glycosylase inhibitors and herbicides (Fig. 2) [24,25]. Thus, the presence of fused isoxazoline with δ-lactone in the structure may enhance the cytotoxic activity. Also, a saturation of C—C double bond of α, β-unsaturated δ-lactone due to cycloaddition in the fused form of a bicyclic molecule may remove the potential threat of, off targeting by nucleophilic amino acids at different receptors by Michael type addition was our thought process [26].

In the present work, the synthesis of novel isoxazoline derivatives of Goniodiol diacetate (**2**) (fused bicyclic pyranone isoxazoline derivatives) has been carried out. The regioselectivity/ regiospecificity of the synthesized derivatives has been confirmed using 1D, 2D NMR spectroscopy and single-crystal XRD. Further, these observed regioselectivities are also validated by analyzing frontier molecular orbitals (FMO) of participating dipoles and dipolarophiles using DFT (Density functional theory) studies. Eleven novel derivatives are synthesized from different aldoximes with electron-donating and withdrawing groups on the aromatic benzene ring. The in vitro anti-cancer activities of all the derivatives are reported against human breast cancer (MDA-MB-231), ovarian cancer (SKOV3), prostate cancer (PC-3) and colon cancer (HCT-15) cell lines along with normal cell lines HEK 293. Cell cycle analysis and Annexin V/PI assay are also performed on selected molecules to ascertain the anti-cancer pathway. Further, the physico-chemical properties like lipophilicity and hydrophilicity are in situ calculated for the synthesized compounds using Schrödinger software.

2. Result & discussion

2.1. Chemistry and regiomer confirmation

1,3-dipolar cycloaddition of nitrile oxides to alkenes is a method of choice for generating isoxazoline compounds with better yields and possible predictability of regioisomer formation [27–29]. In the present work, new isoxazoline derivatives were synthesized from the isolated known Goniodiol-7-monoacetate (**1**) molecule using 1,3- dipolar cycloaddition reaction [20–22]. Goniodiol-7-monoacetate was isolated from the ethyl acetate extract of *Goniothalamus wynaadensis* Bedd. Goniodiol-7-monoacetate was subjected to acetylation using acetic anhydride in the presence of base pyridine leading to Goniodiol diacetate (**2**) as shown in Scheme-1. The relative stereochemistry at the chiral centers of Goniodiol diacetate was found to be 6R,7R,8R [30,31].

This Goniodiol diacetate (**2**) was further subjected to 1, 3 - dipolar cycloaddition with different aldoximes to yield novel isoxazoline derivatives of Goniodiol diacetate, i.e. **3a** to **3 k** (Scheme 1). Various aryl and aliphatic aldoximes, shown in Table 1, were synthesized from their respective aldehydes using well-documented procedures of treatment with hydroxylamine hydrochloride in the presence of a base [32]. The methanolic solution of these individual aldoximes was added dropwise to the cold solution (0–5 °C) containing 0.1% trifluoroacetic acid (TFA), a stoichiometric quantity of iodobenzene diacetate and compound (**2**). The dropwise addition of aldoxime ensured quantitative conversion of aldoximes to nitrile oxide in the reaction, which in turn undergoes 1,3-dipolar cycloaddition with compound (**2**), leading to novel isoxazoline derivatives (**3a** to **3 k**) [33–36].

A total of eleven novel isoxazoline derivatives were synthesized with quantitative yield as a single regioisomer, as displayed in Table 1. In a few substrates, entry 3, 5, 10 & 11, the 1,3 - dipolar cycloaddition reaction between the aldoxime and Goniodiol-diacetate furnished a minor mixture of products which was minorly evident in ^{1}H NMR spectra. In order to ascertain the presence of diastereomers in the reaction mixture, the reversed phase-high performance liquid chromatography (RP-HPLC) was performed using an UFLC Shimadzu HPLC system equipped with binary LC-20 CE pumps, a SIL-20 AC autosampler and an SPD-20A detector (Fig. 3). In brief, 100 µL of 0.1 M solution of the reaction mixture were injected using the autosampler, using a Luna 5 µm PFP (2) 100 Å phenomenix C-18 column (250 mm × 4.6 mm), and monitored at 226 and 280 nm.

The linear gradient of acetonitrile containing 0.1% TFA and HPLC grade water was used as the mobile phase. The area under the curve was estimated using the LabSolutions software provided by the manufacturer. With respect to the area under the curve of a known concentration of **3a** and **3e**, the concentration of **3a** and **3e** in test solutions was estimated. The RP-HPLC elution profile illustrates a single peak for **3a** and **3e** at 13.55 min and 12.75 min, respectively. A minor peak was observed in **3e** compound having elution at 12.35 min, indicating that there is a possibility of diastereomers with the ratio of 94.36%**:** 3.11%. The attempts to collect minor diastereomer in the pure form and confirm the
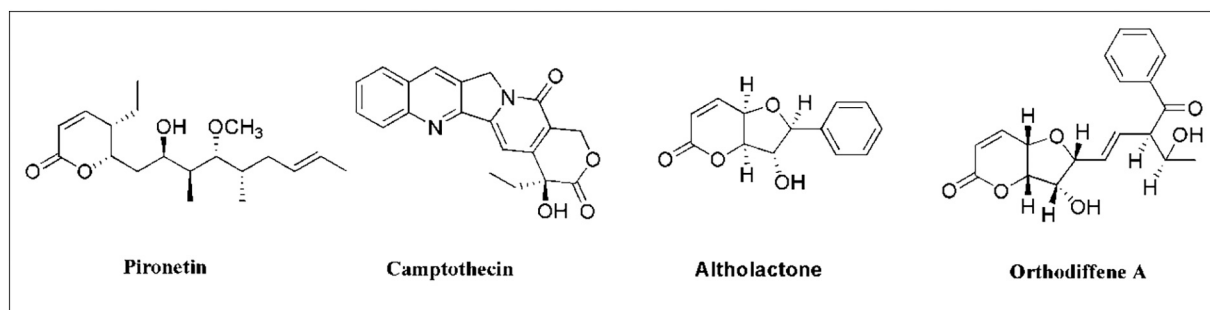

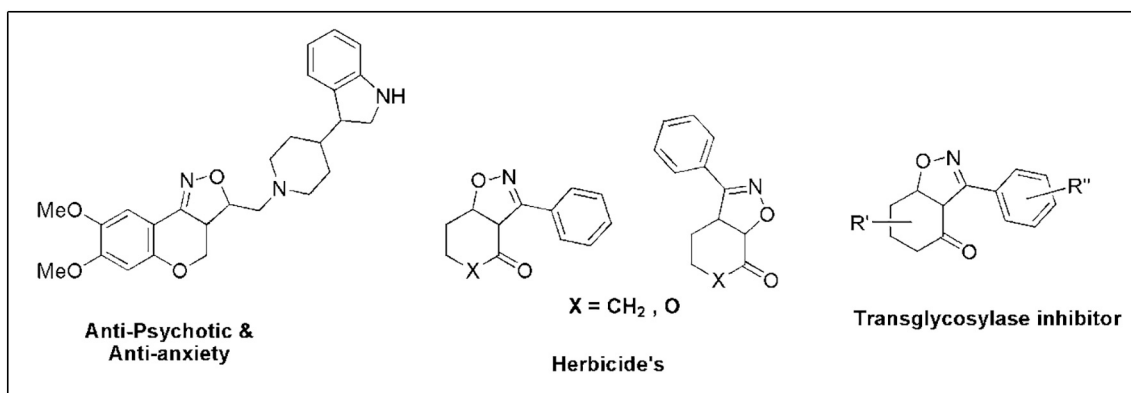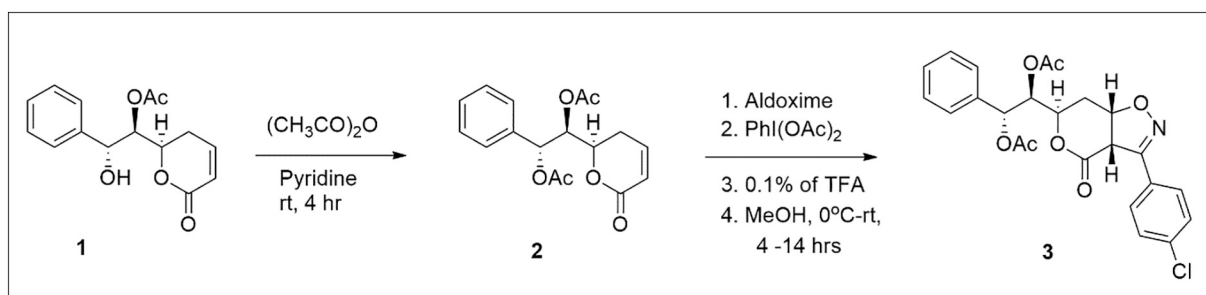**Fig. 1.** Cytotoxic lactones isolated from nature.

Fig. 2. Bioactive fused isoxazolines.

Scheme 1. Synthesis of Goniodiol-diacetate derivatives. Reagents and conditions; (a) Acetic anhydride, pyridine, rt., 4 h, (Yield- 99%). (b) Aldoxime, 0.1% TFA, Iodobenzene diacetate, MeOH, 0 °C-rt, 4 h − 14 h (Yield- 53-89%).

structure were unfortunately futile.

The structure of product **3a** was elucidated by 1D and 2D NMR analysis. ^{1}H and ^{13}C NMR spectra of **3a** revealed that the signals relating to H5, H6, H7 & H8 remained largely undisturbed. The profound shifting of chemical shift for H3 and H4 from δ 6.03 and δ 6.85 in compound **2** to δ 4.72 and δ 5.26, respectively, in the ^{1}H NMR, along with the upfield shift of C3 & C4 signals from δ 121.4 & δ 144.1 to δ 53.0 and δ 78.4, respectively in ^{13}C NMR indicated clearly the formation of isoxazoline ring. The relative positions of Hydrogens attached to respective Carbons were confirmed by [1]H—^{1}H COSY (Correlated spectroscopy) and HMBC (Heteronuclear multiple bond correlation) experiments, while the positions of Carbon signals were confirmed by HSQC (Heteronuclear single quantum coherence) experiment. The coupling constant of 10.8 Hz between H3 and H4 confirmed the *cis* relation between H3 & H4, consistent with the observation and principles of cycloaddition reactions. The regioisomer in which the Oxygen of the nitrile oxide attached to the β- Carbon, i.e., C4 of the α, β-unsaturated-δ-lactone, is anticipated to be a major diastereomer due to the favorable, Large-Large and Small-Small atomic orbital coefficient bonding interactions in the HOMO-LUMO (Highest occupied molecular orbital-Lowest unoccupied molecular orbital) orbital interaction. This indeed was observed in all the reactions in the present series. The H3 signal at δ 4.72 with doublet was shielded as anticipated, compared to the H4 signal at δ 5.26 with a doublet of triplet, deshielded due to the attachment to electronegative Oxygen. The regioisomer was further confirmed by the NOESY (Nuclear overhauser effect spectroscopy) experiment, where H3 showed a strong correlation to H2' of Ar—Cl. The H8, H7 & H6 correlating to each other in the NOESY spectrum were unperturbed. Interestingly, there was no correlation found between H4 & H6 and also no correlation between H3 & H6 in the NOESY, while H3 & H4 were strongly correlated. The NOESY spectra supported the regioisomer structure depicted in Fig. 4 (a), where H3 & H4 are *cis* to each other and probably away from H6 or not in the same plane. To our astonishment,
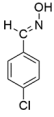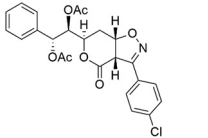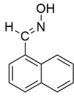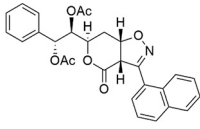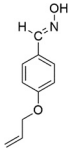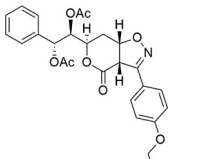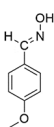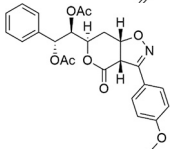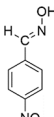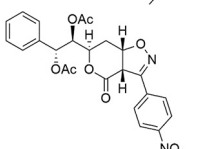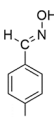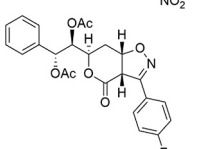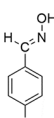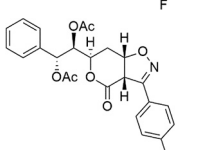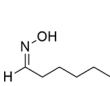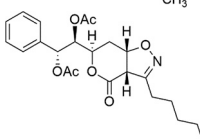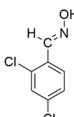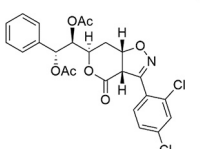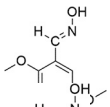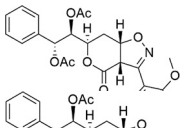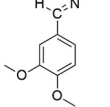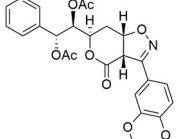
we found a single regioisomer in which the Oxygen of the nitrile oxide attached to the β- Carbon, i.e. C4 of the α, β-unsaturated-δ- lactone as the product and the reaction was regiospecific in this regard. But, in few cases like entries 3, 5, 10 & 11, ^{1}H NMR displayed a slight mixture of diastereomers which may be other stereoisomers of **3c**, **3e**, **3j** & **3 k** where both the protons at C3 & C4 are in α orientation but *cis* to each other. These diastereomers could not be purified and confirmed by spectroscopy due to the poor bioavailability of Goniodiol-7-monoacetate (**1**) to be isolated.

To find the best conformation of the selected compound **3a**, the compound was drawn in a 2D sketcher of Maestro Materials Science 3.4.012 platform of Schrödinger software. The Minimization panel was used to obtain the energy-minimized structure of the compound. Further, this minimized structure was taken for the conformational search in the same platform. The conformational search panel was used to set up a conformational search for the molecule with default panel settings provided by the Maestro Materials Science 3.4.012 platform of Schrödinger software. Eight different conformers of the molecule were obtained as an output of the conformational search. The conformer having the lowest potential energy has been shown in Fig. 4 (b), which was precisely matching with experimentally determined/ recorded crystal structure in Fig. 5. The structure was unambiguously confirmed by the single-crystal structure of **3a**, as shown in Fig. 5.

2.2. FMO interaction studies by DFT

In order to understand further on the regioselectivities of the reaction, theoretical studies were carried out on compound (**2**) as a sample. In the reaction, in situ generated nitrile oxide acts as dipole while compound (**2**) acts as dipolarophile. The formation of regiospecific isoxazoline products has been explained by frontier molecular orbital interactions. All calculations were done using Gaussian16, Revision B.01 software at B3LYP 6-31G (d.p.) level [37]. Analytical frequencies have

Table 1

Isoxazoline derivatives of Goniodiol diacetate by 1,3- dipolar cycloaddition reactions.

Entry	Aldoxime	Product(s)	Isomer	Isolated Yield in %	Reaction time in hours
01			**3a** 100: 00	69	4
02			**3b** 100: 00	83	6
03			**3c** 77: 23	53	12
04			**3d** 100: 00	53	14
05			**3e** 94.36: 5.64	75	4
06			**3f** 100: 00	89	4
07			**3 g** 100: 00	71	4
08			**3 h** 100: 00	60	4
09			**3i** 100: 00	85	4
10			**3j** 86.94: 13.06	63	14
11			**3 k** 85.11: 14.89	63	14
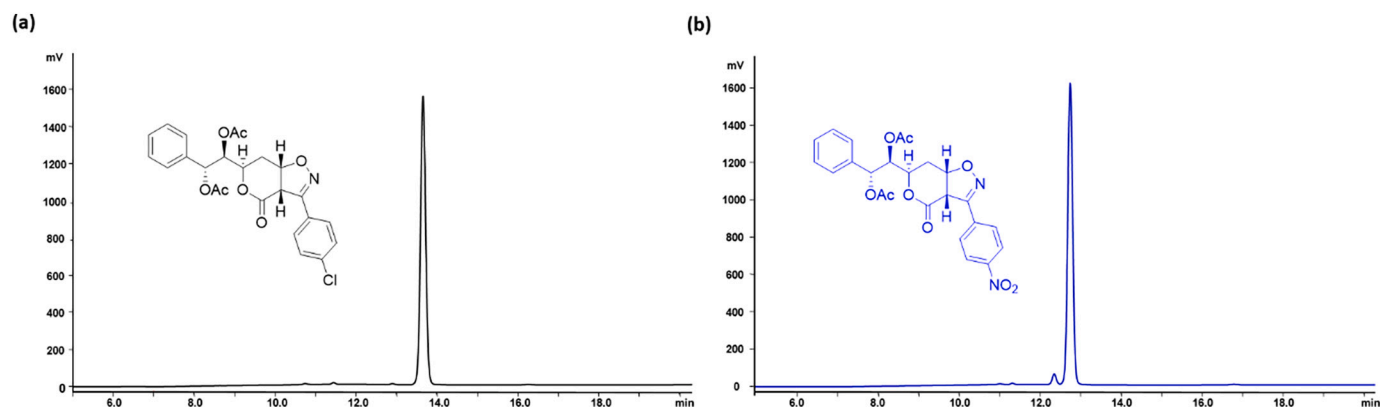
Fig. 3. RP-HPLC elution profiles for the selected compounds, a) **3a** using gradient method with water and acetonitrile solvent system; b) **3e** using gradient method with water and acetonitrile solvent system.
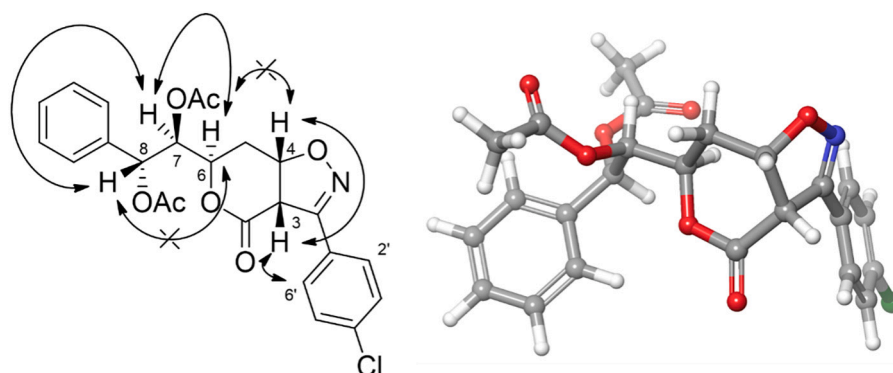
Fig. 4. (a) NOESY correlation for compound **3a** (b) Energy minimized conformer of compound **3a**.
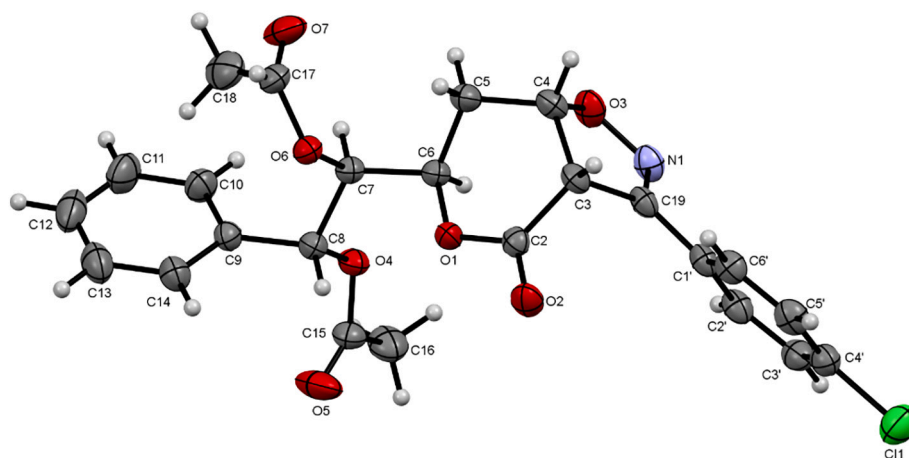
Fig. 5. ORTEP diagram for the crystal structure of compound **3a**.

been evaluated to confirm that the optimized geometries are minimum on the respective potential energy surface. The extraction of contribution from groups of atoms in molecular orbitals has been performed using GaussSum 3.0 software [38].

Frontier molecular orbitals (FMO) have been used to predict the possible mechanism that occurs at the molecular level for selected molecules **3a** and **3e**. The regioselective reaction between *para*-substituted benzaldehyde oxime and α, β-unsaturated δ-lactone, i.e. Goniodiol diacetate (**2**) via 1,3- dipolar cycloaddition has been analyzed. The in-situ generated nitrile oxides from respective aldoximes are rearranged to ionic forms; both —Cl and –NO$_2$ substituted aryl aldoximes are considered in ionized forms and studied as nitrile oxides of 4-chlorobenzaldehyde oxime (**A**) and 4-nitrobenzaldehyde oxime (**B**), respectively (Scheme 2).

The FMO correlation diagram in Fig. 6 shows that the orbital pairs HOMO$_{\overline{A}}$LUMO$_2$ and HOMO$_{\overline{B}}$LUMO$_2$ are separated with 4.90 eV and 5.54 eV, respectively. The substitution of electron-withdrawing –NO$_2$ group on *the para* position of oxime (**B**) results in stabilization of FMO compared to (**A**) [39]. Thus, according to Woodward and Hoffmann's principle of conservation of orbital symmetry and FMO theory, the reaction between (**A**) and (**2**) is more favored than between (**B**) and (**2**) [40]. On the other hand, HOMO-4$_2$ and LUMO$_B$ have a 5.02 eV gap.

Scheme 2. Selected examples for the calculation of Frontier molecular orbital correlation.

Fig. 6. Frontier molecular orbital correlation diagram for the compounds **A**, **2** and **B**.

However, an inspection of FMO of (**A**) and (**B**) reveals that the *para* substitution has a less significant effect on electron density distribution within the molecule. This behavior has been further supported by natural population analysis (NPA), as shown in Table 2. Table 2 provides NPA and coefficients of atomic orbitals in FMO for atoms participating in 1,3 dipolar cycloaddition reactions. Here, compound (**2**) is a dipolarophile, while compounds (**A**) & (**B**) are found to be dipoles.

To be noted, the coefficients of atomic orbitals of C and O [reactive centers of oximes (nitrile oxide)] in FMO significantly differed between (**A**) and (**B**). In case of HOMO, the coefficients of C and O are found to be 8 and 16 for (**A**) while 13 and 21 for (**B**). The atomic orbital coefficient in the case of α, β-unsaturated carbon of δ-lactone compound (**2**) in LUMO$_2$ is 39 for β carbon (C4) and 19 for α carbon (C3). This suggests that the interaction between O—C4 and C—C3 is preferred between compounds (**A**) and (**2**), which also is 'Large-Large' and 'Small-Small' interaction with respect to atomic orbital coefficient participating in the new bond formation as per the Houk's ru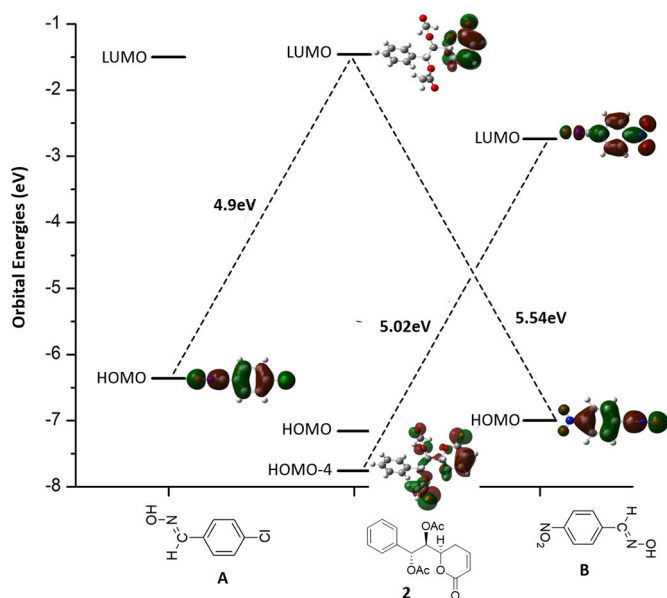le [41]. These interactions are favoring a high yield of regioisomer for the reaction between (**A**) and (**2**). In the case of (**B**) and (**2**), less energy gap for HOMO-4$_2$ and LUMO$_B$ allows participation in reaction along with HOMO$_B$ and LUMO$_2$. Though, the atomic orbital coefficients of reactive centers in LUMO$_B$ are not large enough to elucidate the preferred reaction path. This allows the formation of the mixture of regioisomers for the reaction between the electron-withdrawing group containing (**B**) and (**2**) [42,43].

2.3. Cytotoxic studies against cancer cell lines

The chemically novel isoxazoline derivatives of Goniodiol diacetate were subjected to the cytotoxicity study (MTT assay) to analyze the half-maximal effective concentration (EC$_{50}$). Four contrasting human cancer cell lines named MDA-MB-231, SKOV3, PC-3, HCT-15, and one normal human cell line, i.e., HEK 293, were used for the study. All the derivatives, when compared to that of a standard drug (Vincristine), gave a tuned response, i.e., more or less equal to the standard. From Table 3, it is clear that all the derivatives were inhibiting cancer cells without harming the normal cell line with EC$_{50}$ <10 μM. It may be due to the reason that cancer cells are metabolically more active and continuously dividing irrespective of the normal cell lines, thus engulfing the drug/compound more potentially.

Interestingly the new fused bicyclic pyranone isoxazoline derivatives

Table 2
Coefficients of selected atomic orbitals in frontier molecular orbitals and natural population analysis (NPA in eV) of dipolarophile and dipoles.

Molecule	Coefficient	HOMO-4	LUMO	NPA
Compound 2	C4	9	39	−0.144
	C3	12	19	−0.358
Molecule	Coefficient	HOMO	LUMO	NPA
A	C	8	16	0.218
	O	16	4	−0.381
B	C	13	3	0.215
	O	21	2	−0.378

Table 3

Cytotoxic activity of compounds (**2**, **3a-3 k**) against SKOV3, MDA-MB-231, PC-3, HCT-15 cancer cell lines and HEK 293 cell line.

Compound	$EC_{50} \pm SD$ in μM				
	SKOV3	MDA-MB-231	PC-3	HCT-15	HEK-293
2	8.80 ± 1.89	9.79 ± 1.10	8.6 ± 0.96	8.84 ± 1.28	>100
3a	9.35 ± 1.25	7.03 ± 2.13	9.7 ± 1.63	8.83 ± 1.52	>100
3b	8.94 ± 2.01	8.17 ± 1.14	9.7 ± 1.28	8.19 ± 2.20	>100
3c	8.12 ± 0.92	7.78 ± 0.85	8.7 ± 1.02	7.80 ± 1.48	>100
3d	9.18 ± 1.41	7.34 ± 0.63	9.0 ± 1.08	8.49 ± 1.98	>100
3e	10.80 ± 1.92	9.40 ± 0.32	10.7 ± 0.66	8.06 ± 0.36	>100
3f	6.52 ± 1.19	6.50 ± 1.10	8.6 ± 0.66	6.46 ± 0.90	>100
3 g	6.83 ± 1.15	6.88 ± 1.56	8.1 ± 0.52	10.98 ± 0.12	>100
3 h	9.52 ± 0.82	9.42 ± 1.24	5.9 ± 1.04	9.47 ± 0.23	>100
3i	7.95 ± 0.95	6.19 ± 1.27	9.0 ± 1.78	6.42 ± 0.84	>100
3j	8.63 ± 1.36	8.42 ± 0.66	9.5 ± 0.45	9.75 ± 0.47	>100
3 k	9.17 ± 1.59	8.14 ± 1.66	10.1 ± 0.58	8.08 ± 1.96	>100
Vincristine	9.02 ± 1.28	7.00 ± 1.19	7.59 ± 1.33	6.14 ± 1.39	>100

SD-Standard deviation.

have not lost the anti-cancer activity compared to the Goniodiol diacetate (**2**). This suggests that the presence of conjugated C—C double bond in the δ-lactone of Goniodiol diacetate may not be essential for cytotoxicity. The presence of saturated lactone seems to be vital for the activity. The variation of dipolarophile oxime by size, by electronic parameters (electron releasing groups or electron-withdrawing groups on aryl ring) (**3a-3 k**), have little influence on improving the cytotoxicity values, suggests that the binding pocket at the probable target site may be large or open. So, more chemical space can be explored with the synthesis of the fused bicyclic heterocyclic derivatives on this natural molecule for improving bioactivity. Thus, we can say that all these derivatives were promising in inhibiting cancer cell proliferation. Among all compounds, **3 f** has been selected for in-depth study for its effect on the apoptosis and cell-cycle analysis as it was one of the most potent cytotoxic molecules with 6.83 μM and 6.88 μM activity against SKOV3 & MDA-MB-231.

2.4. Apoptosis studies and discussion of compound 3 f on MDA-MB-231 cancer cell lines

The apoptosis induced by compound **3 f** was determined by annexin V/PI staining assay. This annexin V/PI assay is a proven method to differentiate the live, necrotic, early apoptotic, and late apoptotic cells, as shown in Fig. 7. MDA-MB-231 cells were treated with compound **3 f** for 24 h at indicated concentrations (3.44 μM, 6.88 μM and 13.76 μM). The results obtained after the treatment with compound **3 f** showed a dose-dependent response with respect to the percentage of total apoptotic cells (early and late apoptotic) 2.94% at 3.44 μM, whereas the percentage of total apoptotic cells was 5.01% at 6.88 μM and but declined to 3.14% at 13.76 μM in comparison to Vincristine that has shown 26.6% at 7.00 μM. However, cell proliferation was arrested mainly due to necrosis with 24.45%, 32.23%, and 34.78%, at 3.44 μM, 6.88 μM, and 13.76 μM dose concentrations.

The cell cycle analysis was performed to assess at which phase of cell cycle compound **3 f** is arresting the cell growth. The breast cancer cell

lines-MDA-MB-231 were treated with compound **3 f** for 24 h at indicated concentrations. The compound **3 f** showed 12.88%, 16.55% and 17.67% of cell accumulation at 3.44 μM, 6.88 μM, and 13.76 μM concentrations, respectively, in the S phase (Fig. 8), keeping cell control (CC) as a reference where it showed 11.88% cell accumulation at S phase. Whereas Vincristine showed 69.37% at 7.00 μM concentration in the G2/M phase and CC showed 16.01% accumulation. The results clearly indicated that compound **3 f** arrested the cell proliferation at the early phase of the cell cycle, i.e. S phase and standard Vincristine arrests at the last phase, i.e. G2/M phase.

2.5. ADME studies

Lipinski's rule of five is considered as a thumb rule while predicting the oral bioavailability of a probable drug molecule [44]. This rule is considered not applicable to the compounds of the natural product origin. The synthesized compounds were analyzed for their oral bioavailability and drug-likeness by Schrodinger's QikProp module. This module gives in silico values for Log P & Log S, as shown in Table 4. Log P is an indicator of partition coefficient or lipophilicity of compounds, and Log S is an indicator of solubility of compounds in water. Both these parameters are essential pharmacokinetic properties for a compound or a drug to cross the cell membrane. All the synthesized compounds **3a-3 K** have a molecular weight <500 Da except **3i**, and all these have Log P values in the range of 1.511 to 2.785, which is <5 which satisfies Lipinski's rule (Table 4). Log S values for **3a-3 k** were in the range − 4.446 to −2.982, which is an acceptable range for a drug candidate for its hydrophilicity. The number of hydrogen bond donors for **3a-3 k** were zero, and hydrogen bond acceptors were <10 or around it, which is acceptable as per Lipinski's rule (Table 4).

3. Conclusion

In conclusion, a total of eleven novel isoxazoline derivatives of Goniodiol diacetate (fused bicyclic pyranone isoxazoline derivatives) were synthesized with quantitative yield as a single regioisomer by 1,3 - dipolar cycloaddition reaction with different aldoximes. The regiospecific product formed was confirmed by NOESY study and single-crystal X-ray diffraction. The regiospecificity of the product formation was further explained unambiguously by coefficients of selected atomic orbitals in frontier molecular orbitals and natural population analysis (NPA in eV) of dipolarophile, i.e., Goniodiol diacetate, and dipoles, i.e., aldoximes by DFT studies. All the derivatives have demonstrated anti-cancer activity selectively to MDA-MB-231, SKOV3, PC-3, and HCT-15 cell lines with $EC_{50} < 10$ μM. Additionally, Annexin V/PI assay and cell cycle analysis on selected potent compound **3 f** exhibited tuned apoptotic response & necrosis compared to standard Vincristine. Also, it showed cell growth arrest in the S phase, which is the early phase. All the synthesized molecules were found to comply with Lipinski's rule of five for the oral bioavailability of a candidate drug molecule. We can conclude from the results that novel fused bicyclic pyranone isoxazolines are relatively less observed in the chemical space & biological space and need to be explored further for diverse bioactivity. The current derivatives are selectively potent anti-cancer compounds, and a more in-depth study of these compounds is essential to develop a promising anti-cancer candidate.

4. Experimental

4.1. General

All melting points were recorded in open capillaries on a digital melting/ boiling point apparatus. Commercially available reagents and solvents were used. HPLC MeOH Merck Mumbai was used for Monitoring the reactions. All reactions were carried out at 0 °C to room temperature, and chromatography was performed with 230–400 mesh
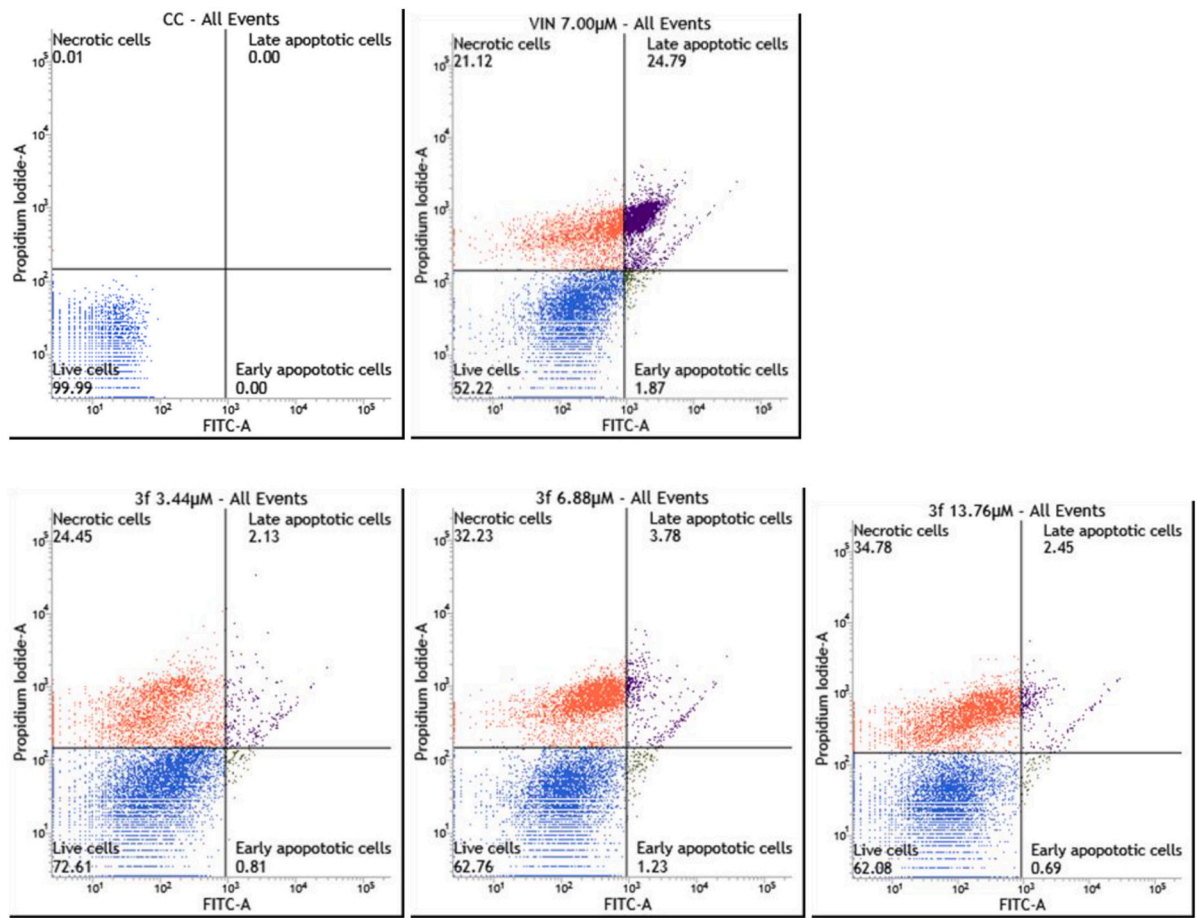
a
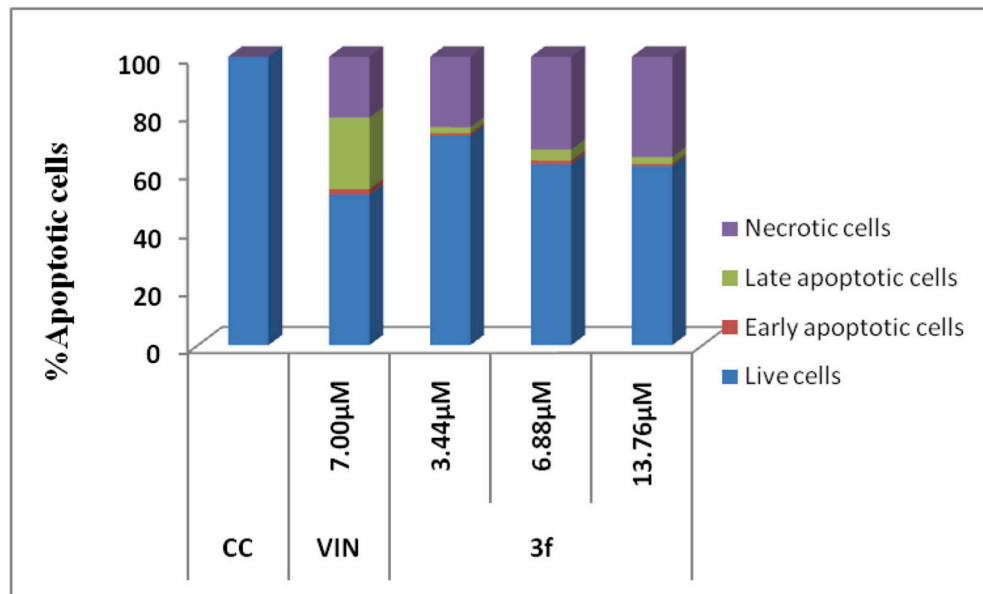
b

Fig. 7. a) MDA-MB-231 cells were treated with compound **3 f** at 3.44, 6.88 and 13.76 μM and Vincristine at 7.00 μM for 24 h. Annexin V-FITC/PI dye assay determining the percentage of apoptotic cells. **b)** The bar graph representation showing the apoptotic cell population.
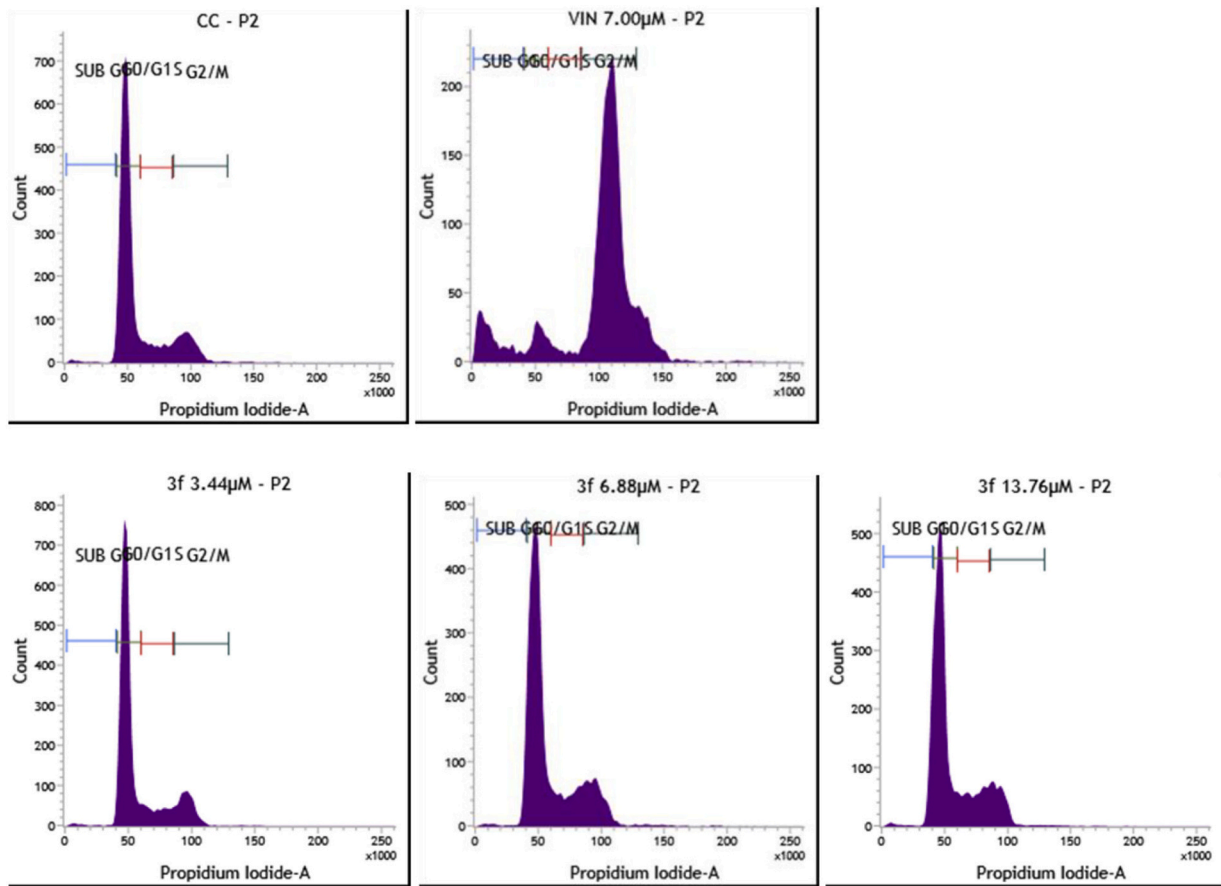
a
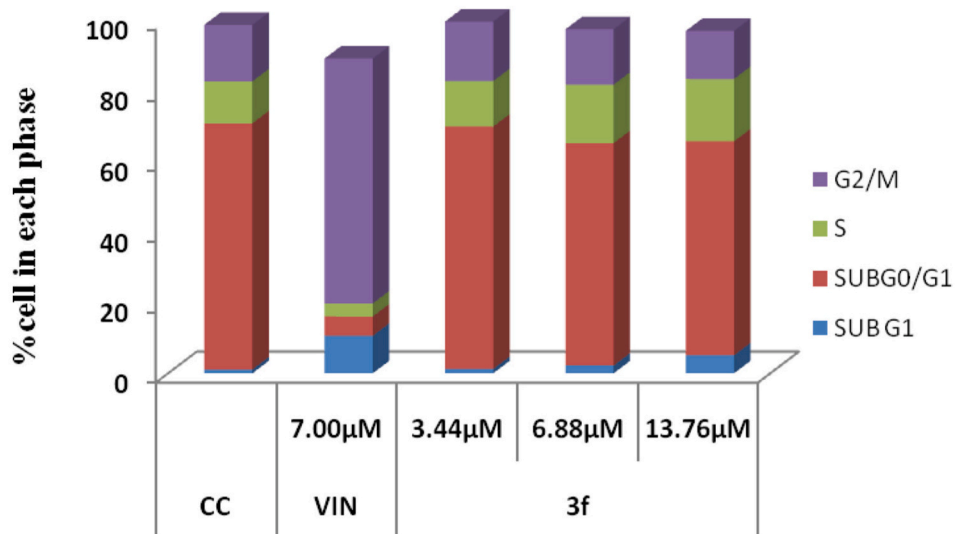
b

Fig. 8. a) Flow cytometric analysis of MDA-MB-231 cells after the treatment with compound **3 f** (3.44 μM, 6.88 μM and 13.76 μM) and Vincristine (7.00 μM) for 24 h, where CC represents cell control. **b)** The bar graph representation of cell cycle analysis for compound **3 f.**

Table 4
Pharmacokinetic parameters of compounds **3a-3 k** as determined by QikProp application of Schrödinger software.*

Compound	Mol. Wt.	Log P	Log S	HB donor	HB acceptor
3a	471.893	2.785	−3.918	0	10
3b	487.508	3.22	−4.194	0	10
3c	493.512	3.115	−4.197	0	10
3d	467.474	2.286	−3.195	0	10
3e	482.446	1.511	−3.156	0	10
3f	455.439	2.518	−3.523	0	10
3 g	451.475	2.594	−3.74	0	10
3 h	431.485	2.408	−2.982	0	10
3i	506.338	3.248	−4.446	0	10
3j	497.501	2.502	−3.407	0	11
3 k	497.501	2.321	−3.282	0	11
Vincristine	409.23	2.87	−4.93	1	5

* HB-Hydrogen bond.

silica gel Merck, Mumbai. ^{1}H NMR spectra were recorded on Bruker 500 or 400 MHz spectrometers, and ^{13}C NMR spectra were recorded at 125 MHz, respectively. Chemical shifts are reported as δ values (ppm) relative to internal standard tetramethylsilane in CDCl$_3$. HRMS (ESI) were recorded on Fourier transform ESI-HRMS. FT-IR PerkinElmer® spectra were recorded.

4.2. Preparation of Goniodiol diacetate (2)

(1S,2R)-1-(6-oxo-3,6-dihydro-2H-pyran-2-yl)-2-phenylethane-1,2-diyl diacetate (**2**)

Goniodiol-7-monoacetate (**1**) (20 mg) was taken in a 25 mL round bottom (R. B.) flask. To this, excess acetic anhydride (10 eq) was added. The reaction mixture was allowed to stir, and the compound (**1**) dissolved completely. To this reaction mixture, a stoichiometric quantity of pyridine (2 eq) was added. The reaction mixture was allowed to stir and was monitored for completion by TLC. On completion of the reaction, the reaction mixture was quenched with saturated copper sulphate solution to remove unreacted pyridine. It was further extracted with water and ethyl acetate. The organic layer was separated, dried over sodium sulphate and evaporated under a vacuum. The pure product compound **2** (Goniodiol diacetate) was separated by filter column chromatography. The yield was quantitative.

White solid, mp = 155-157 °C; $[\alpha]_D^{25}$ +110.41 (c = 0.0017, CHCl$_3$); R$_f$ 0.45 (EtOAc-Hexane, 1: 1); ^{1}H NMR (500 MHz, CDCl$_3$): δ 7.33 (m, 5H), 6.85 (dddd, J = 9.75, 5.5, 2.5 Hz, 1H), 6.07 (d, J = 8.5 Hz, 1H), 6.02 (d, J = 2.0 Hz, 1H), 5.35 (dd, J = 8.5, 2.5 Hz, 1H) 4.76 (dddd, J = 10.75, 5, 2.5 Hz, 1H) 2.41–2.31 (m, 2H), 2.08 (s, 3H), 1.82 (s, 3H); ^{13}C NMR (500 MHz, CDCl$_3$): δ 169.7, 168.9, 162.8, 144.1, 136.4, 128.6, 128.4, 127.4, 121.4, 74.6, 73.5, 72.3, 26.0, 20.9, 20.2. HRMS (ESI): calcd for C$_{17}$H$_{19}$O$_6$N [M + H] 319.11, found 319.1173.

4.3. General procedure for the synthesis of new isoxazoline derivatives of Goniodiol diacetate (2)

In a clean 50 mL round bottom flask (Diacetoxyiodo)benzene (DIB) (1.2 eq) was taken, which was allowed to dissolve in HPLC grade methanol. To this one drop, Trifluoroacetic acid (TFA) was added at 0 °C. In another beaker, compound (**2**), i.e., Goniodiol diacetate (1.0 eq), was dissolved in methanol. The compound (**2**) solution was added slowly to the reaction mixture in round bottom flask, maintaining 0 °C. The reaction mixture was allowed to stir for about 5–10 min. To this reaction mixture, a solution of derivative of pre-prepared oxime (1.5 eq) in methanol was added slowly dropwise for about half an hour, maintaining 0 °C. The reaction was monitored for completion by TLC. After completion of the reaction, methanol was evaporated under a vacuum, and the compound was extracted with ethyl acetate and water. The organic layer was dried over sodium sulphate and concentrated to get the desired compound. The pure compound (**3a** to **3 k**) was separated by

column chromatography. Isolated yield ranged from 53% to 89%.

(1S,2R)-1-(3-(4-chlorophenyl)-4-oxo-4,6,7,7a-tetrahydro-3aH-pyrano[3,4-d]isoxazol-6-yl)-2-phenylethane-1,2-diyl diacetate (**3a**)

White solid; Yield: 69%; mp 125-128 °C; R$_f$ 0.44 (EtOAc-Hexane, 2: 3); IR (cm^{-1}): ν_{max} 2926, 2854, 1740, 1595, 1494, 1370, 1213, 700.; ^{1}H NMR (400 MHz, CDCl$_3$): δ 7.84 (dd, J = 9.2, 2.4 Hz, 2H), 7.43 (dd, J = 9.25, 2.5 Hz, 2H), 7.33–7.30 (m, 5H), 5.92 (d, J = 8.8 Hz, 1H), 5.33 (dd, J = 8.8, 2.4 Hz, 1H), 5.26 (dt, J = 10.8, 5.6 Hz, 1H) 4.84 (dt, J = 11.6, 3.6 Hz, 1H), 4.72 (d, J = 10.8 Hz, 1H), 2.30–2.23 (m, 1H), 2.0–1.8(m, 1H), 1.96 (s, 3H), 1.81 (s, 3H); ^{13}C NMR (400 MHz, CDCl$_3$): δ 169.5, 168.9, 163.8, 152.0, 137.2, 136.2, 129.2, 128.87, 128.82, 128.4, 127.3, 125.7, 78.4, 73.3, 72.9, 72.1, 53.0, 30.5, 20.8, 20.2. HRMS (ESI): calcd for C$_{24}$H$_{22}$ClO$_7$N [M + H]$^+$ 472.11, found 472.11469.

(1S,2R)-1-(3-(naphthalen-1-yl)-4-oxo-4,6,7,7a-tetrahydro-3aH-pyrano[3,4-d]isoxazol-6-yl)-2-phenylethane-1,2-diyl diacetate (**3b**)

Butter yellow shade solid; Yield: 83%; mp 112-115 °C; R$_f$ 0.45 (EtOAc- Hexane, 2: 3); IR (cm^{-1}): ν_{max} 2923, 2853, 1739, 1212, 1039, 774, 700; ^{1}H NMR (500 MHz, CDCl$_3$): δ 8.66 (d, J = 8.5 Hz, 1H), 7.94 (d, J = 8.5 Hz, 1H), 7.89 (d, J = 7.5 Hz, 1H), 7.79 (d, J = 7 Hz, 1H), 7.59–7.52 (m, 3H), 7.31–7.25 (m, 5H), 5.86 (d, J = 9 Hz, 1H) 5.33 (m, 2H), 5.05 (d, J = 11 Hz, 1H), 4.99 (d, J = 12 Hz, 1H), 2.31–2.28 (m, 1H), 2.08–1.92 (m, 1H), 1.82 (s, 3H), 1.75 (s, 3H); ^{13}C NMR (500 MHz, CDCl$_3$): δ 169.4, 168.8, 163.8, 152.1, 136.3, 134.0, 131.6, 130.6, 128.9, 128.7, 128.4, 127.6127.3, 127.1, 126.3, 125.5, 124.9, 123.3, 76.7, 73.2, 72.9, 72.0, 55.7, 31.5, 20.5, 20.2. HRMS (ESI): calcd for C$_{28}$H$_{26}$O$_7$N [M + H]$^+$ 488.16, found 488.16977.

(1S,2R)-1-(3-(4-(allyloxy)phenyl)-4-oxo-4,6,7,7a-tetrahydro-3aH-pyrano[3,4-d]isoxazol-6-yl)-2-phenylethane-1,2-diyl diacetate (**3c**)

Golden yellow oil; Yield: 53%;R$_f$ 0.5 (EtOAc- Hexane, 2: 3); IR (cm^{-1}): ν_{max} 2922, 2853, 1737, 1605, 1513, 1371, 1216, 701; ^{1}H NMR (500 MHz, CDCl3): δ 7.82 (d, J = 9 Hz, 2H), 7.40–7.26 (m, 5H), 6.93 (d, J = 9 Hz, 2H), 6.04 (m, 1H), 5.90 (d, J = 9 Hz, 1H), 5.45 (dd, J = 17.25, 1.5 Hz, 1H), 5.32 (dddd, J = 11, 2.5 Hz, 2H), 5.22 (dt, J = 7, 2 Hz, 1H), 4.86 (d, J = 10.5, 1.5 Hz, 1H), 4.74 (d, J = 11 Hz, 1H), 4.57 (d, J = 5 Hz, 2H), 2.24–1.9 (m, 2H), 1.93 (s, 3H), 1.81 (s, 3H); ^{13}C NMR (500 MHz, CDCl$_3$): δ 169.4, 168.9, 164.3, 160.7, 152.2, 136.3, 132.7, 129.1, 128.7, 128.4, 127.3, 119.7, 118.0, 114.8, 77.8, 73.2, 72.8, 72.1, 68.8, 53.5, 30.8, 20.7, 20.2. HRMS (ESI): calcd for C$_{27}$H$_{28}$O$_8$N [M + H]$^+$ 494.17, found 494.17968.

(1S,2R)-1-(3-(4-methoxyphenyl)-4-oxo-4,6,7,7a-tetrahydro-3aH-pyrano[3,4-d]isoxazol-6-yl)-2-phenylethane-1,2-diyl diacetate (**3d**).

Golden brown shade solid; Yield: 53%; mp 117-119 °C; $[\alpha]_D^{25}$ -11.48 (c = 0.0023, CHCl$_3$); R$_f$ 0.53 (EtOAc- Hexane, 2: 3); IR (cm^{-1}): ν_{max} 2923, 2853, 1738, 1607, 1515, 1371, 1253, 1214, 1043, 701; ^{1}H NMR (500 MHz, CDCl$_3$): δ 7.83 (dd, J = 9.5, 3 Hz, 2H), 7.30 (m, 5H), 6.94 (dd, J = 9.5, 3 Hz, 2H), 5.90 (d, J = 9 Hz, 1H), 5.33 (dd, J = 9, 2.5 Hz, 1H), 5.22 (dt, J = 11.74, 2 Hz, 1H), 4.88 (dt, J = 10, 2 Hz, 1H), 4.75 (d, J = 11 Hz, 1H), 3.84 (s, 3H), 2.24–2.04 (m, 2H), 1.93 (s, 3H) 1.80 (s, 3H); ^{13}C NMR (500 MHz, CDCl$_3$): δ 169.4, 168.8, 164.3, 161.7, 152.2, 136.3, 129.1, 128.7, 128.4, 127.4, 127.3, 119.6, 114.2, 77.7, 73.2, 72.8, 72.1, 55.3, 53.6, 30.8, 20.7, 20.2. HRMS (ESI): calcd for C$_{25}$H$_{26}$O$_8$N [M + H]$^+$ 468.16, found 468.16489.

(1S,2R)-1-(3-(4-nitrophenyl)-4-oxo-4,6,7,7a-tetrahydro-3aH-pyrano[3,4-d]isoxazol-6-yl)-2-phenylethane-1,2-diyl diacetate (**3e**)

Brownish beige yellow solid; Yield: 75%; mp 105-107 °C; $[\alpha]_D^{25}$ -5.83 (c = 0.0024, CHCl$_3$); R$_f$ 0.51 (EtOAc- Hexane, 2: 3); IR (cm^{-1}): ν_{max} 2923, 2853, 1738, 1520, 1213, 1039, 700; ^{1}H NMR (500 MHz, CDCl$_3$): δ 8.27 (dd, J = 8.5, 2.5 Hz, 2H), 8.12 (dd, J = 8.5, 2.5 Hz, 2H), 7.34 (m, 5H), 5.94 (d, J = 6.5 Hz, 1H), 5.34 (m, 2H), 4.83 (dd, J = 10.4, 2 Hz, 1H), 4.74 (d, J = 10.8 Hz, 1H), 2.34–2.31 (m, 1H), 2.08 (s, 3H), 2.07–2.03 (m, 1H), 1.99 (s, 3H); ^{13}C NMR (500 MHz, CDCl$_3$): δ 169.6, 169.1, 163.5, 151.8, 149.0, 136.1, 133.3, 128.9, 128.6, 128.2, 127.3, 124.1, 79.3, 73.2, 73.0, 72.2, 52.3, 29.8, 21.1, 20.3; HRMS (ESI): calcd for C$_{24}$H$_{21}$O$_9$N$_2$ [M + H]$^+$ 481.13, found 481.12570.

(1S,2R)-1-(3-(4-fluorophenyl)-4-oxo-4,6,7,7a-tetrahydro-3aH-

pyrano[3,4-*d*]isoxazol-6-yl)-2-phenylethane-1,2-diyl diacetate **(3f)**

Medium golden yellow solid; Yield: 89%; mp 130-132 °C; R$_f$ 0.66 (EtOAc- Hexane, 2: 3); IR (cm^{-1}): ν_{max} 2924, 2853, 1733, 1602, 1514, 1375, 1215, 1036, 699; ^{1}H NMR (400 MHz, CDCl$_3$): δ 7.91 (dt, $J = 8.8$, 2 Hz, 2H), 7.31 (m, 5H), 7.13 (dt, $J = 8.8$, 2 Hz, 2H), 5.93 (d, $J = 8.8$ Hz, 1H), 5.34 (dd, $J = 8.8$, 2.4 Hz, 1H), 5.26 (dt, $J = 11.8$, 2 Hz, 1H), 4.86 (dt, $J = 11.6$, 1.6 Hz, 1H), 4.84 (d, $J = 10.8$ Hz, 1H), 2.27–2.23 (m, 1H), 1.96 (s, 3H), 1.94–1.89 (m, 1H), 1.81 (s, 3H); ^{13}C NMR (400 MHz, CDCl$_3$): δ 169.5, 168.9, 164.0, 151.9, 136.2, 129.7, 129.71, 128.8, 128.4, 127.3, 116.1, 116.0, 78.2, 73.2, 72.9, 72.1, 53.2, 30.5, 20.8, 20.2. HRMS (ESI): calcd for C$_{24}$H$_{22}$FO$_7$N [M + H]$^+$ 456.14, found 456.14401.

(1*S*,2*R*)-1-(4-oxo-3-(p-tolyl)-4,6,7,7a-tetrahydro-3aH-pyrano[3,4-*d*] isoxazol-6-yl)-2-phenylethane-1,2-diyl diacetate **(3 g)**

Light yellow solid; Yield: 71%; mp 135-137 °C; $[\alpha]_{D}^{25}$ -27.61 (c = 0.0021, CHCl$_3$); R$_f$ 0.52 (EtOAc- Hexane, 2: 3); IR (cm^{-1}): ν_{max} 2924, 2854, 1735, 1372, 1213, 1183, 1033, 1060; ^{1}H NMR (400 MHz, CDCl$_3$): δ 7.76 (d, $J = 8.4$ Hz, 2H), 7.31 (m, 5H), 7.24 (d, $J = 8.4$ Hz, 2H), 5.91 (d, $J = 8.8$ Hz, 1H), 5.32 (dd, $J = 12.8$, 2.8 Hz, 1H), 5.24 (dt, $J = 11$, 2.4 Hz, 1H), 4.87 (dt, $J = 10.2$, 2.4 Hz, 1H), 4.77 (d, $J = 10.8$ Hz, 1H), 2.38 (s, 3H), 2.25–2.17 (m, 2H) 1.93 (s, 3H), 1.82 (s, 3H); ^{13}C NMR (400 MHz, CDCl$_3$): δ 169.5, 168.8, 164.2, 152.6, 141.4, 136.3, 129.5, 128.7, 128.4, 127.4, 127.3, 124.3, 77.9, 73.3, 72.9, 72.1, 53.5, 30.9, 21.4, 20.8, 20.2. HRMS (ESI): calcd for C$_{25}$H$_{25}$O$_7$N [M + H]$^+$ 452.16, found 452.16998.

(1*S*,2*R*)-1-(4-oxo-3-pentyl-4,6,7,7a-tetrahydro-3aH-pyrano[3,4-*d*] isoxazol-6-yl)-2-phenylethane-1,2-diyl diacetate **(3 h)**

Yellowish brown oil; Yield: 60%; R$_f$ 0.60 (EtOAc- Hexane, 2: 3); IR (cm^{-1}): ν_{max} 2925, 2856, 1741, 1459, 1371, 1215, 1043, 699; ^{1}H NMR (400 MHz, CDCl$_3$): δ 7.33 (m, 5H), 6.01 (d, $J = 8.8$ Hz, 1H), 5.31 (d, $J = 10$ Hz, 1H), 5.03 (d, $J = 11.2$ Hz, 1H) 4.74 (d, $J = 10.8$ Hz, 1H), 4.21 (d, $J = 10.8$ Hz, 1H), 2.41 (m, 2H) 2.07 (s, 3H), 1.80 (s, 3H), 1.74–1.26 (m, 8H), 0.91 (t, $J = 3.2$ Hz, 3H); ^{13}C NMR (400 MHz, CDCl$_3$): δ 169.4, 168.9, 163.8, 154.7, 136.2, 128.7, 128.4, 127.4, 76.0, 73.2, 72.7, 72.1, 55.2, 31.2, 30.2, 26.3, 25.7, 22.2, 20.9, 20.1, 13.8. HRMS (ESI): calcd for C$_{23}$H$_{29}$O$_7$N [M + H]$^+$ 432.20, found 432.20139.

(1*S*,2*R*)-1-(3-(2,4-dichlorophenyl)-4-oxo-4,6,7,7a-tetrahydro-3aH-pyrano[3,4-*d*]isoxazol-6-yl)-2-phenylethane-1,2-diyl diacetate **(3i)**

Butter yellow shade oil; Yield: 85%; R$_f$ 0.56 (EtOAc- Hexane, 2: 3); IR (cm^{-1}): ν_{max} 2955, 1739, 1371, 1213, 1041, 700; ^{1}H NMR (400 MHz, CDCl$_3$): δ 7.51 (s, 1H), 7.38–7.32 (m, 7H), 5.99 (d, $J = 8.8$ Hz, 1H), 5.35 (dd, $J = 9$, 2.4 Hz, 1H), 5.29 (dt, $J = 10.8$, 4.4 Hz, 1H), 4.90 (d, $J = 12.2$ Hz, 2H), 2.32–2.28 (m, 1H), 2.09 (s, 3H), 1.99–1.94 (m, 1H), 1.79 (s, 3H); ^{13}C NMR (400 MHz, CDCl$_3$): δ 169.5, 168.9, 164.0, 151.9, 136.2, 129.78, 129.71, 128.8, 128.4, 127.3, 116.1, 116.0, 78.2, 73.2, 72.9, 72.1, 53.2, 30.5, 20.8, 20.2. HRMS (ESI): calcd for C$_{24}$H$_{21}$Cl$_2$O$_7$N [M + H]$^+$ 506.07, found 506.07584.

(1*S*,2*R*)-1-(3-(2,5-dimethoxyphenyl)-4-oxo-4,6,7,7a-tetrahydro-3aH-pyrano[3,4-*d*]isoxazol-6-yl)-2-phenylethane-1,2-diyl diacetate **(3j)**

Clear viscous oil; Yield: 63%; R$_f$ 0.5 (EtOAc- Hexane, 2: 3); IR (cm^{-1}): ν_{max} 2923, 2853, 1740, 1497, 1371, 1213, 1040, 701; ^{1}H NMR (400 MHz, CDCl$_3$): δ 7.32 (m, 5H), 6.96 (m, 2H), 6.90 (d, $J = 2.2$ Hz, 1H) 5.92 (d, $J = 9.2$ Hz, 1H), 5.34 (dd, $J = 9.2$, 2.4 Hz, 1H), 5.22 (dt, $J = 11$, 2 Hz, 1H), 4.97 (d, $J = 11.2$ Hz, 1H), 4.87 (dt, $J = 11.8$, 1.6 Hz, 1H), 3.82 (s, 3H), 3.77 (s, 3H), 2.20 (m, 1H), 2.05 (s, 3H), 1.88 (m, 1H), 1.79 (s, 3H); ^{13}C NMR (400 MHz, CDCl$_3$): δ 169.0, 163.9, 153.6, 152.2, 136.4, 132.9, 128.7, 128.4, 127.4, 121.5, 117.3, 116.8, 115.6, 112.9, 77.6, 73.3, 72.5, 72.2, 56.2, 55.8, 54.9, 31.0, 20.8, 20.1. HRMS (ESI): calcd for C$_{26}$H$_{27}$O$_9$N [M + H]$^+$ 498.17, found 498.17496.

(1*S*,2*R*)-1-(3-(3,4-dimethoxyphenyl)-4-oxo-4,6,7,7a-tetrahydro-3aH-pyrano[3,4-*d*]isoxazol-6-yl)-2-phenylethane-1,2-diyl diacetate **(3 k)**

Clear viscous oil; Yield: 63%; R$_f$ 0.35 (EtOAc- Hexane, 2: 3); IR (cm^{-1}): ν_{max} 2936, 1738, 1515, 1371, 1213, 1022, 701; ^{1}H NMR (400 MHz, CDCl$_3$): δ 7.50 (m, 2H), 7.30 (m, 5H), 6.90 (d, $J = 8.4$ Hz, 1H), 5.93 (d, $J = 8.8$ Hz, 1H), 5.34 (d, $J = 8.4$ Hz, 1H), 5.24 (d, $J = 10.8$ Hz, 1H), 4.88 (d, $J = 11.6$ Hz, 1H), 4.75 (d, $J = 10.8$ Hz, 1H), 3.97 (s, 6H), 2.24

(m, 1H), 2.07 (m, 1H), 1.94 (s, 3H), 1.82 (s, 3H); ^{13}C NMR (400 MHz, CDCl$_3$): δ 169.8, 169.1, 164.6, 152.3, 151.4, 149.2, 136.4, 129.1, 129.0, 127.6, 121.4, 119.8, 110.9, 109.5, 77.9, 73.2, 72.9, 72.1, 55.9 (Twice intensity), 53.5, 30.8, 29.9, 21.2, 20.2. HRMS (ESI): calcd for C$_{26}$H$_{27}$O$_9$N [M + H]$^+$ 498.17, found 498.17563.

4.4. Anti-cancer activity methodology

4.4.1. Cell culture

The cell lines for breast cancer (MDA-MB-231), prostate cancer (PC-3), colon cancer (HCT-15), ovarian cancer (SKOV3) and human embryonic kidney cell lines (HEK-293) were purchased from National Centre for Cell Science (NCCS) -Pune, India. The cells were cultured in media such as Dulbecco's modified eagle's medium (DMEM), Roswell Park memorial institute (RPMI-1640) supplemented with 10% (*V/V*) Fetal bovine serum, 100 units/ ml of penicillin, and streptomycin. All cell lines were cultured and incubated at 37 °C humidified atmosphere with 5% CO$_2$. Test compounds were dissolved in DMSO to prepare a stock solution for biological experiments.

4.4.2. Cytotoxicity study

The chemically synthesized novel isoxazoline derivatives of Goniodiol diacetate were evaluated for their cytotoxicity along with positive standard Vincristine against five human cell lines viz., human breast cancer MDA-MB-231, ovarian cancer SKOV3, prostate cancer PC-3 and colon cancer HCT-15 cell lines along with normal cell lines HEK-293 after 24 h of drug treatment by MTT assay. Briefly, 96 well plates were seeded with 1×10^4 cells/well (100 μL each) and incubated at 37 °C for 24 h with 5% CO$_2$. Later these seeded cells were treated with 20 μL of serially diluted compounds (starting from 100 μM up to 0.78 μM) isoxazoline derivatives of Goniodiol diacetate and positive control Vincristine. The treated plates were again incubated at 37 °C for another 24 h with a constant supply of 5% CO$_2$.

After the completion of 24 h of incubation, 20 μL per well MTT [3-(4,5-dimethylthiazol-2-yl)-2,5-diphenyl tetrazolium bromide] reagent (5 mg/mL PBS) was added, and plates were again incubated at 37 °C for 2 h. Post incubation, around 70 μL of untransformed MTT was removed and replaced with an equal volume of DMSO to dissolve formazan crystals formed by the MTT reagent. Finally, the density of cells was observed by the absorbance studied at 570 nm using a spectrophotometer. The cytotoxicity of the hybrids was calculated, acknowledging cell controls as 100% viability.

%Viability = OD of treated cells/OD of untreated cells x100

4.4.3. Annexin V-FITC/PI staining assay

The apoptotic assay was determined using Annexin V/FITC detection kit (Sigma Aldrich) by a reported method. MDA-MB-231 cells were seeded 2×10^5 cells/ well in a 6-well plate and incubated for 24 h with 5% CO$_2$ at 37° C. The cells were then treated with Vincristine (7.00 μM) and compound **3 f** at indicated concentrations (3.44 μM, 6.88 μM and 13.76 μM) for 24 h at 37° C with 5% CO$_2$. After 24 h of incubation, media was discarded, cells were washed with PBS and were gently trypsinized. Cells were resuspended in 1 mL of 1× binding buffer and incubated with 5 μL of Annexin V-FITC and 10 μL of propidium iodide for 15 min at room temperature in the dark condition. Analysis was carried out by flow cytometer (FACS Verse, Becton-Dickinson, USA).

4.4.4. Cell cycle analysis

DNA content of the cell cycle progression was studied by a reported method. MDA-MB-231 cells were incubated 2×10^5 cells/ well in 6-well plates with incomplete media (Serum-free) for 24 h. After 24 h, incomplete media was replaced with complete media with or without standard Vincristine (7.00 μM) and compound **3 f** at indicated concentrations (3.44 μM, 6.88 μM and 13.76 μM) and incubated for another 24 h. The cells were washed thrice with PBS, harvested, fixed with ice-cold

70% ethanol (200 µL) and stored at -20°C for 30 min. After fixation of cells, they were resuspended with 50 µL of RNase (0.1 mg/mL) and incubated at 37°C for 30 min. Finally, cells were stained with 100 µL of propidium iodide (50 µg/mL), incubated for 30 min in ice-cold dark conditions and then DNA content was measured by using BD FACS Verse flow cytometer (Becton-Dickinson, USA).

Author's contribution

Mr. Doddabasappa Talimarada did the bench work of synthesis & isolation of the molecule. Collection of data.

Dr. Akanksha Sharma did the analysis work with spectroscopic data & biological data along with Mr. Doddabasappa Talimarada.

Mr. Mahesh G Wakhradkar & *Dr. Krishna Chaitanya Gunturu did the DFT studies and wrote the DFT part in the manuscript.

Prof. Sunder N. Dhuri worked on the crystal structure determination and data collection for crystallography.

Dr. Venkata Narayanan Naranammalpuram Sundaram worked in Manuscript writing & correction.

*Dr. Harish Holla planned the research work, manuscript writing & correction and coordination with all involved in the work.

Declaration of Competing Interest

The authors declare that they have no known competing financial interests or personal relationships that could have appeared to influence the work reported in this paper.

Acknowledgement

Appendix A. Supplementary data

Supplementary data to this article can be found online at https://doi.org/10.1016/j.fitote.2022.105316.

References

[1] G.M. Cragg, D.J. Newman, K.M. Snader, Natural products in drug discovery and development, J. Nat. Prod. 60 (1) (1997) 52–60, https://doi.org/10.1021/np9604893.

[2] D.J. Newman, G.M. Cragg, K.M. Snader, Natural products as sources of new drugs over the period 1981-2002, J. Nat. Prod. 66 (7) (2003) 1022–1037, https://doi.org/10.1021/np030096l.

[3] M. Gordaliza, Natural products as leads to anticancer drugs, Clin. Transl. Oncol. Off Publ. Fed. Spanish Oncol. Soc. Natl Cancer Inst. Mex. 9 (12) (2007) 767–776, https://doi.org/10.1007/s12094-007-0138-9.

[4] D.J. Newman, G.M. Cragg, Natural products as sources of new drugs over the last 25 years, J. Nat. Prod. 70 (3) (2007) 461–477, https://doi.org/10.1021/np068054v.

[5] D.J. Newman, G.M. Cragg, Natural products as sources of new drugs over the nearly four decades from 01/1981 to 09/2019, J. Nat. Prod. 83 (3) (2020) 770–803, https://doi.org/10.1021/acs.jnatprod.9b01285.

[6] A. Sharma, P. Sharma, S. Singh, T.B. Karegoudar, H. Holla, Evaluation of leaves of Goniothalamus wynaadensis Bedd. for inhibition of metabolic viability of cancer cells & antimicrobial efficacy, Eur J Integr Med. 32 (2019) 101000, https://doi.org/10.1016/j.eujim.2019.101000.

[7] K.A. Sujana, R.G. Vadhyar, A new species of goniothalamus (Annonaceae) from the western ghats of Tamil Nadu, India, Taiwania. 65 (2) (2020) 176–180, https://doi.org/10.6165/tai.2020.65.176.

[8] Hooker Joseph Dalton, No TitleJ. D. Hooker Assisted by Various Botanists, Published under the authority of the secretary of state for India in council, 1885.

[9] P. Oudhia, No TitleMedicinal Orchid Habenaria furcifera Lindl, in: Based Herb Formul used Blood Relat Dis Indian Tradit Heal Pankaj Oudh Ethnobot Surv 1990-2012, 2022. Published online 2013.

[10] P. Oudhia, Some Popular Important Tags of Pankaj Oudhia related to Biodiversity and Traditional Healing Blood Cancer and Prostate Cancer. Http://WwwPankajoudhiaCom/Home-Page/Imptags2Pdf. Published online 2013, 2022, p. 654.

[11] P. Oudhia, Goniothalamus wynaadensis Based Tribal Medicines for Diabetes, 2022. Published online 2014.

[12] M. Shahzad Aslam, M. Syarhabil Ahmad, A. Soh Mamat, M. Zamharir Ahmad, F. Salam, Goniothalamus: phytochemical and ethnobotanical review, Recent Adv Biol Med. 02 (July) (2016) 34, https://doi.org/10.18639/rabm.2016.02.292264.

[13] A. Kaur, S. Kaur, R. Jandrotia, et al., Parthenin—a Sesquiterpene lactone with multifaceted biological activities: insights and prospects, Molecules. 26 (17) (2021), https://doi.org/10.3390/molecules26175347.

[14] D.M. Reddy, N.A. Qazi, S.D. Sawant, et al., Design and synthesis of spiro derivatives of parthenin as novel anti-cancer agents, Eur. J. Med. Chem. 46 (8) (2011) 3210–3217, https://doi.org/10.1016/j.ejmech.2011.04.030.

[15] B.A. Shah, R. Kaur, P. Gupta, et al., Structure-activity relationship (SAR) of parthenin analogues with pro-apoptotic activity: development of novel anti-cancer leads, Bioorg. Med. Chem. Lett. 19 (15) (2009) 4394–4398, https://doi.org/10.1016/j.bmcl.2009.05.089.

[16] T. Usui, H. Watanabe, H. Nakayama, et al., The anticancer natural product Pironetin selectively targets Lys352 of α-tubulin, Chem. Biol. 11 (6) (2004) 799–806, https://doi.org/10.1016/j.chembiol.2004.03.028.

[17] M. Yoshida, Y. Matsui, Y. Ikarashi, T. Usui, H. Osada, H. Wakasugi, Antiproliferating activity of the mitotic inhibitor pironetin against vindesine- and paclitaxel-resistant human small cell lung cancer H69 cells, Anticancer Res. 27 (2) (2007) 729–736.

[18] H. Holla, A. Sharma, P. Bhat, D. Shinde, B. Das, Phytochemistry Letters Two new substituted polychiral 5, 6-dihydro- α -pyrones from Orthosiphon di ff usus and molecular docking studies, Phytochem. Lett. 22 (May) (2017) 21–26, https://doi.org/10.1016/j.phytol.2017.08.006.

[19] H. Holla, Y. Srinivas, A. Majhi, et al., Novel cytotoxic constituents of Orthosiphon diffusus q, Tetrahedron Lett. 52 (1) (2011) 49–52, https://doi.org/10.1016/j.tetlet.2010.10.140.

[20] Y.C. Wu, C.Y. Duh, F.R. Chang, et al., The crystal structure and cytotoxicity of goniodiol-7-Monoacetate from goniothalamus amuyon, J. Nat. Prod. 54 (4) (1991) 1077–1081, https://doi.org/10.1021/np50076a024.

[21] V. Jäger, V. Buß, W. Schwab, Syntheses via isoxazolines III. Diastereoselective synthesis of γ-amino-alcohols with 2 and 3 chiral centres, Tetrahedron Lett. 19 (34) (1978) 3133–3136, https://doi.org/10.1016/S0040-4039(01)94963-9.

[22] R.P. Tangallapally, D. Sun, Rakesh, et al., Discovery of novel isoxazolines as anti-tuberculosis agents, Bioorg. Med. Chem. Lett. 17 (23) (2007) 6638–6642, https://doi.org/10.1016/j.bmcl.2007.09.048.

[23] J.I. Andrés, J. Alcázar, J.M. Alonso, et al., Discovery of a new series of centrally active tricyclic isoxazoles combining serotonin (5-HT) reuptake inhibition with α2-adrenoceptor blocking activity, J. Med. Chem. 48 (6) (2005) 2054–2071, https://doi.org/10.1021/jm049619s.

[24] C.J. Easton, G.A. Heath, C.M.M. Hughes, et al., Electrochemical and yeast-catalysed ring-opening of isoxazoles in the synthesis of analogues of the herbicide Grasp®, J Chem Soc Perkin 1 (10) (2001) 1168–1174, https://doi.org/10.1039/b008081k.

[25] R.C.F. Jones, A. Chatterley, R. Marty, W.M. Owton, M.R.J. Elsegood, Isoxazole to oxazole: a mild and unexpected transformation, Chem. Commun. 51 (6) (2015) 1112–1115, https://doi.org/10.1039/c4cc07999j.

[26] D. Mulliner, D. Wondrousch, G. Schüürmann, Predicting Michael-acceptor reactivity and toxicity through quantum chemical transition-state calculations, Org. Biomol. Chem. 9 (24) (2011) 8400–8412, https://doi.org/10.1039/c1ob06065a.

[27] I.N.N. Namboothiri, N. Rastogi, Isoxazolines from nitro compounds: synthesis and applications, Synth Heterocycles via Cycloaddit I (2022) 1–44, https://doi.org/10.1007/7081_2007_101. Published online 2008.

[28] A.P. Kozikowski, The Isoxazoline route to the molecules of nature, Acc. Chem. Res. 17 (12) (1984) 410–416, https://doi.org/10.1021/ar00108a001.

[29] M. Christl, R. Huisgen, Reaktionen der Knallsaure mit ungesättigten Verbindungenz, Chem Ber. 106 (1973) 3291–3311.

[30] C. Zhao, Z. Ye, Z. Ma, Xiong, et al., A general strategy for diversifying complex natural products to polycyclic scaffolds with medium-sized rings, Nat. Commun. 10 (1) (2019), https://doi.org/10.1038/s41467-019-11976-2.

[31] S. Majhi, D. Das, Chemical derivatization of natural products: semisynthesis and pharmacological aspects- a decade update, Tetrahedron. 78 (xxxx) (2021) 131801, https://doi.org/10.1016/j.tet.2020.131801.

[32] A. Sharma, D. Talimarada, U.P. Yadav, et al., Design and synthesis of new tubulin polymerization inhibitors inspired from Combretastatin A-4: an anticancer agent, ChemistrySelect. 5 (37) (2020) 11560–11572, https://doi.org/10.1002/slct.202003170.

[33] B. Das, H. Holla, G. Mahender, K. Venkateswarlu, B.P. Bandgar, A convenient method for the preparation of benzopyrano- and furopyrano-2-isoxazoline derivatives using hypervalent iodine reagents, Synthesis-Stuttgart 10 (2005) 1572–1574, https://doi.org/10.1055/s-2005-865314.

[34] B.A. Mendelsohn, S. Lee, S. Kim, F. Teyssier, V.S. Aulakh, M.A. Ciufolini, Oxidation of oximes to nitrile oxides with hypervalent iodine reagents, Org. Lett. 11 (7) (2009) 1539–1542, https://doi.org/10.1021/ol900194v.

[35] T. Jen, B.A. Mendelsohn, M.A. Ciufolini, Oxidation of α-oxo-oximes to nitrile oxides with hypervalent iodine reagents, J. Organomet. Chem. 76 (2) (2011) 728–731, https://doi.org/10.1021/jo102241s.

[36] B. Das, H. Holla, G. Mahender, J. Banerjee, Reddy M. Ravinder, Hypervalent iodine-mediated interaction of aldoximes with activated alkenes including Baylis-Hillman adducts: a new and efficient method for the preparation of nitrile oxides from aldoximes, Tetrahedron Lett. 45 (39) (2004) 7347–7350, https://doi.org/10.1016/j.tetlet.2004.07.159.

[37] Gaussian 16, Revision B.01, M. J. Frisch, G. W. Trucks, H. B. Schlegel, G. E. Scuseria, M. A. Robb, J. R. Cheeseman, G. Scalmani, V. Barone, G. A. Petersson, H. Nakatsuji, X. Li, M. Caricato, A. V. Marenich, J. Bloino, B. G. Janesko, R. Gomperts, B. Mennucci, H. P. Hratchian, J. V. Ortiz, A. F. Izmaylov, J. L. Sonnenberg, D. Williams-Young, F. Ding, F. Lipparini, F. Egidi, J. Goings, B. Peng, A. Petrone, T. Henderson, D. Ranasinghe, V. G. Zakrzewski, J. Gao, N. Rega, G. Zheng, W. Liang, M. Hada, M. Ehara, K. Toyota, R. Fukuda, J. Hasegawa, M. Ishida, T. Nakajima, Y. Honda, O. Kitao, H. Nakai, T. Vreven, K. Throssell, J. A. Montgomery, Jr., J. E. Peralta, F. Ogliaro, M. J. Bearpark, J. J. Heyd, E. N. Brothers, K. N. Kudin, V. N. Staroverov, T. A. Keith, R. Kobayashi, J. Normand, K. Raghavachari, A. P. Rendell, J. C. Burant, S. S. Iyengar, J. Tomasi, M. Cossi, J. M. Millam, M. Klene, C. Adamo, R. Cammi, J. W. Ochterski, R. L. Martin, K. Morokuma, O. Farkas, J. B. Foresman, and D. J. Fox, Gaussian, Inc., Wallingford CT, 2016.

[38] A. Allouche, Software news and updates Gabedit — a graphical user interface for computational chemistry softwares, J. Comput. Chem. 32 (2012) 174–182, https://doi.org/10.1002/jcc.

[39] M. Weil, W. Eisenhardt, ks = 1.26. 1973;1, Soc AC. (1971) 4092–4094.

[40] T. Deb, J. Tu, R.M. Franzini, Mechanisms and substituent effects of metal-free bioorthogonal reactions, Chem. Rev. 121 (12) (2021) 6850–6914, https://doi.org/10.1021/acs.chemrev.0c01013.

[41] K.N. Houk, A.P. Marchand Rel, Pericyclic Reactions 1(Chapter 4), Acad Press New York, 1977, pp. 182–266.

[42] T.M. Gilbert, Computational prediction of regiospecificity in the [4+2] Diels-Alder cyclizations between the iminoborane (F 3C) 3C-B≡N-(t- Bu) and substituted cis-butadienes, Organometallics. 24 (26) (2005) 6445–6449, https://doi.org/10.1021/om050754s.

[43] G. Galvani, R. Lett, C. Kouklovsky, Regio- and stereochemical studies on the nitroso-diels-alder reaction with 1,2-disubstituted dienes, Chem. - A Eur. J. 19 (46) (2013) 15604–15614, https://doi.org/10.1002/chem.201302905.

[44] C.A. Lipinski, F. Lombardo, B.W. Dominy, P.J. Feeney, Experimental and computational approaches to estimate solubility and permeability in drug discovery and development settings, Adv. Drug Deliv. Rev. 64 (SUPPL) (2012) 4–17, https://doi.org/10.1016/j.addr.2012.09.019.